December, 1993] © *1993 The Chemical Society of Japan* *Bull. Chem. Soc. Jpn.*, ***66***, *3553—3558(1993)* 3553

Discotic Liquid Crystals of Transition Metal Complexes. XVI. Discotic Mesomorphism and Unique Chromism of Bis[1,2-bis(3,4-dialkoxyphenyl)ethanedione dioximato]palladium(II) Complexes[1)]

Kazuchika Ohta,* Mitsuo Moriya, Mayumi Ikejima, Hiroshi Hasebe,
Tetsuya Fujimoto, and Iwao Yamamoto
Department of Functional Polymer Science, Faculty of Textile Science & Technology, Shinshu University, Ueda, 386

(Received April 16, 1993)

Bis[1, 2- bis(3, 4- dialkoxyphenyl)ethanedione dioximato]palladium(II) complexes, (abbreviated $[Pd\{(C_nO)_4dpg\}_2]$; $n=1$—12)have been synthesized and characterized. It was found that each of the $[Pd\{(C_nO)_4dpg\}_2]$ ($n=2$—12) complexes has an enantiotropic discophase (D_{hd}). The clearing points of the $[Pd\{(C_nO)_4dpg\}_2]$ ($n=4$, 8, 12) complexes are higher than those of the corresponding $[Ni\{(C_nO)_4dpg\}_2]$ ($n=4$, 8, 12) complexes. Interestingly, the $[Pd\{(C_nO)_4dpg\}_2]$ complexes exhibit thermochromism and solvatochromism similar to that of $[Ni\{(C_nO)_4dpg\}_2]$ complexes.

The history of the metal glyoximates is long and can be traced back to the year of 1915 when a Russian chemist, Tschugaeff,[2)] first discovered a reaction between nickel salts and the organic compound dimethylglyoxime, which yields the bis(dimethylglyoximato)nickel(II) complex. Since this complex is insoluble in water, dimethylglyoxime has been widely used as a quantitative analytical reagent for nickel. In 1960 Drickamer et at.[3,4)] revealed that bis(glyoximato)metal(II) (metal=Ni, Pd, Pt) complexes, including bis(dimethylglyoximation)nickel(II), exhibit piezochromism due to the nd_{z^2}–$(n+1)p_z$ transition of the metal. The d–p transition is very sensitive to the one-dimensional metal–metal stacking distance and shows a large red shift with increasing pressure.

Recently, Shirotani et al.[5,6)] have precisely inestigated the piezochromism of these bis(gloyoximato)metal(II) complexes. They pointed out a possibility of its application to a pressure indicator. In order to obtain discotic liquid crystals of the bis(glyoximato)metal(II) complexes exhibiting such a unique chromism, we attempted to introduce long-chain-substituents into these core complexes. Recently, we suceeded in synthesizing the bis(octaalkoxy- substituted diphenylglyoximato)nickel(II) complexes, bis[1,2-bis(3,4-dialkoxyphenyl)ethanedione dioximato]nickel(II) (**1**), (abbreviated as $[Ni\{(C_nO)_4dpg\}_2]$; $n=4$, 8, 12; Fig. 1).[7)] It was found that the $[Ni\{(C_nO)_4dpg\}_2]$ ($n=4$, 8, 12) complexes have discotic hexagonal disordered columnar (D_{hd}) mesophases, and that the $[Ni\{(C_nO)_4dpg\}_2]$ ($n=8$, 12) complexes exhibit thermochromism and solvatochromism.[8)] These new characteristics were apparently caused by the introduction of alkoxy chains.

On the other hand, it is well-known that the mesomorphic properties and structures of transition metal complexes as influenced by the central metal. For example, although the bis[*p*-(octyloxy)dithiobenzoato]nickel (II) complex transforms into the [*p*-(octyloxy)-dithiobenzoato] [*p*-(octyloxy)perthiobenzoato]nickel(II) complex during the heating stage, the Pd complex does not;[9)] as another example, although the bis(alkyl-substituted stryldithiolato)nickel(II) and platinum(II) complexes exhibit mesomorphic properties, the Pd complexes do not.[10)] Such different behaviors of these complexes are of particular interest to us.

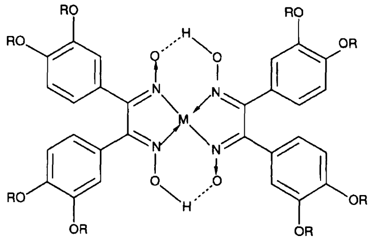

M=Ni, R=C_nH_{2n+1}(n=4,8,12) ········ 1

M=Pd, R=C_nH_{2n+1}(n=1~12) ········ 2

Fig. 1. Formula of the bis(octaalkoxy-substituted diphenylglyoximato)palladium(II) complexes, abbreviated as $1=[Ni\{(C_nO)_4dpg\}_2]$ and $2=[Pd\{(C_nO)_4dpg\}_2]$.

From this viewpoint, we have synthesized the bis[1,2-bis(3,4-dialkoxyphenyl)ethanedione dioximato]-palladium(II) complexes (**2**), (abbreviated as $[Pd\{(C_nO)_4dpg\}_2]$; $n=1$—12; Fig. 1). Contrary to our expectation, the $[Pd\{(C_nO)_4dpg\}_2]$ ($n=2$—12) complexes have an enantiotropic discophase (D_{hd}). The clearing points of the $[Pd\{(C_nO)_4dpg\}_2]$ ($n=4$, 8, 12) complexes are higher than those of the $[Ni\{(C_nO)_4dpg\}_2]$ ($n=4$, 8, 12) complexes. Hence, the discophases of the $[Pd\{(C_nO)_4dpg\}_2]$ complexes have a wider temperature range than do those of the $[Ni\{(C_nO)_4dpg\}_2]$ complexes; further, these two metal complexes give the same discophase. Interestingly, the $[Pd\{(C_nO)_4dpg\}_2]$ complexes also exhibit thermochromism and solvatochromism, as do the $[Ni\{(C_nO)_4dpg\}_2]$ complexes.

In this paper we wish to report on the discotic mesomorphism, thermochromism, and solvatochromism of the $[Pd\{(C_nO)_4dpg\}_2]$ complexes.

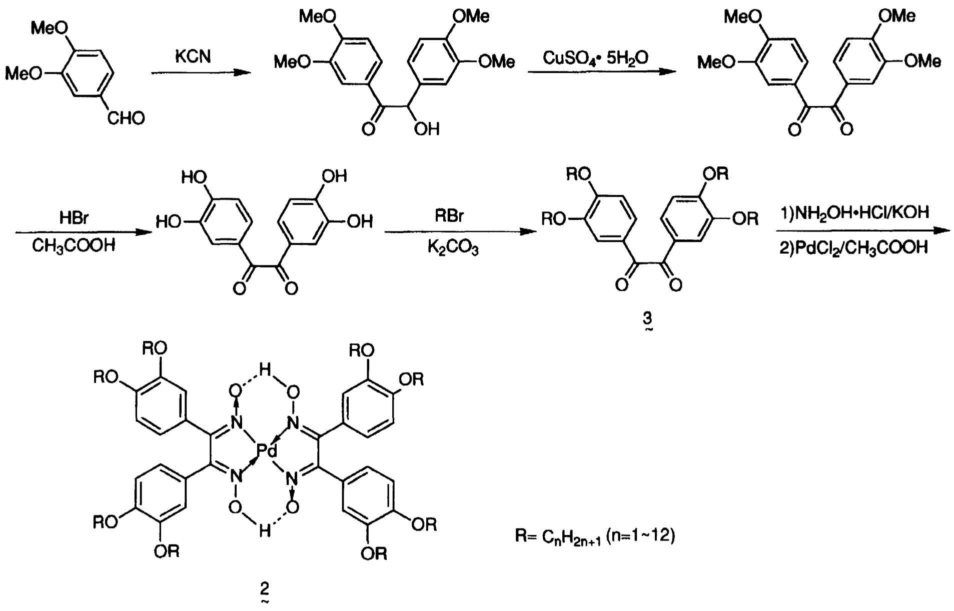

Scheme 1. Synthetic route of the $[Pd\{(C_nO)_4dpg\}_2]$ (n=1—12) complexes 2.

Table 1. Reaction Solvents, Elemental Analysis Data, Yields, Reprecipitation (Recrystallization) Solvents, and the Colors of the $[Pd\{(C_nO)_4dpg\}_2]$ (n=1—12) Complexes

n	Reaction solvent	Elemental analysis (%) Found (Calcd) C	H	N	Yield %	Reprecipitation (recrystallization) solvent	Color
1	Methanol	51.96 (52.40)	4.58 (4.64)	6.37 (6.79)	9.7	Chloroform/Ethyl acetate	Orange
2	Ethanol	55.98 (56.38)	5.69 (5.81)	5.96 (5.98)	7.8	Chloroform/Ethel acetate	Orange
3	Ethanol	59.58 (59.51)	6.70 (6.72)	5.30 (5.34)	17	THF[a)]/Acetone	Orange
4	Methanol : Ethanol=1 : 1	62.00 (62.03)	7.51 (7.46)	4.93 (4.82)	7.8	THF/Acetone	Orange
5	Ethanol	64.35 (64.11)	8.07 (8.07)	4.47 (4.40)	5.2	THF/Acetone	Orange
6	Ethanol	66.12 (65.85)	8.54 (8.58)	4.11 (4.04)	14	THF/Acetone	Orange
7	Ethanol	67.46 (67.33)	8.92 (9.01)	3.61 (3.74)	18	THF/Acetone	Orange
8	Methanol : Ethanol=1 : 1	68.37 (68.61)	9.24 (9.39)	3.48 (3.48)	4.6	THF/Acetone	Orange
9	Ethanol	69.75 (69.72)	9.63 (9.71)	3.22 (3.25)	19	THF/Acetone	Dark red
10	Ethanol	70.91 (70.69)	9.93 (10.00)	2.85 (3.05)	4.3	THF/Acetone	Dark red
11	Ethanol	71.57 (71.55)	10.25 (10.25)	2.88 (2.88)	6.4	THF/Acetone	Dark red
12	Ethanol	72.23 (72.32)	10.47 (10.47)	2.71 (2.72)	6.9	THF/Acetone	Dark red

a) THF=tetrahydrofuran.

Experimental

Synthesis The precursor α-diketone (**3**) was synthesized following our previous method.[7)] The complexes (**2**) were prepared by the reaction of the corresponding α-diketones (**3**) and hydroxylamine hydrochloride in appropriated solvents, followed by a reaction with an ethanol solution of palladium(II) chloride (Scheme 1). After neutralization of the reaction mixture, the target complex (**2**) was obtained as orange or dark-red (liquid) crystals. A representative procedure is given for $[Pd\{(C_{12}O)_4dpg\}_2]$ as follows. In Table 1 are summarized the reaction solvents, elemental analysis data, yields, reprecipitation (recrystallization) solvents, and colors of the $[Pd\{(C_nO)_4dpg\}_2]$ complexes.

Bis[1,2-bis[3,4-bis(dodecyloxy)phenyl]ethanedione dioximato]palladium(II) Complex (2), $[Pd\{(C_{12}O)_4dpg\}_2]$: To 220 ml of ethanol, hydroxylamine hydrochloride (8.68 g, 125 mmol) and 85% purity of potassium hydroxide (8.68 g, 125 mmol) were added. The mixture was vigorously stirred for 30 min and filtered to remove the precipitate. To the filtrate was added 1,2-bis[3,4-bis(dodecyloxy)phenyl]ethanedione (**3**) (2.00 g, 2.12 mmol). Under a nitrogen atmosphere, the mixture was refluxed with stirring for 2 h. To the hot reaction mixture was added palladium(II) chloride (0.16 g, 0.90 mmol) in 5 ml of ethanol. After neutralization with acetic acid, a yellow precipitate was separated out in the reaction mixture. The entire mixture was cooled in an ice-water bath for 1 h, and the yellow sticky precipitate was collected on filter paper. After the precipitate was extracted with chloroform, evaporation of the solvent gave dark-red liquid crystals. Purification was carried out by column chromatography (silica gel, dichloromethane, R_f=0.63) and reprecipitation (recrystallization for n=1—6) by adding acetone into a hot solution of the product in tetrahydrofuran to give 0.15 g (6.9%) of dark-red liquid crystals: ^{1}H NMR ($CDCl_3$) δ=0.87 (24H, t, J=5 Hz, $-CH_3$), 1.25

(160H, m), 3.63 (8H, t, J=5 Hz, -OCH$_2$), 3.90 (8H, t, J=5 Hz, -OCH$_2$), and 6.69—6.91 (12H, m, phenyl); IR (neat), 2940 (alkyl), 2860 (alkyl), and 1600 cm^{-1} (aromatic).

Measurements. The products synthesized here were confirmed by elemental analysis. The phase transition behaviors of these compounds were observed by a polarizing microscope equipped with a heating plate controlled by a thermoregulator (Mettler FP80 and FP82) and were measured with Rigaku Thermoflex TG-DSC differential scanning calorimeter. The temperature-dependent X-ray diffraction measurements of the mesophases were performed using laboratory-made instruments.[11,12] Temperature-dependent electronic spectra were recorded by the technique reported in our previous papers.[8,12] The electrochemical property was determined in a dichloromethane solution containing 0.1 M tetrabutylammonium perchlorate (1 M=1 mol dm^{-3}) as a supporting electrolyte. A cyclic voltammogram was obtained with a Yanagimoto Polarographic Analyzer (P-900) and recorded with a Graphtec X-Y recorder (WX1000). The measurement was made at a glassy carbon working electrode vs. a saturated calomel electrode (SCE). The half-wave potential for the first oxidation of the [Pd{(C$_{12}$O)$_4$dpg}$_2$] complex was +0.95 V.

Results and Discussion

Table 2 summarizes the phase transition behaviors of the [Pd{(C$_n$O)$_4$dpg}$_2$] complexes. As can be seen in this table, each of the [Pd{(C$_n$O)$_4$dpg}$_2$] (n=2—12) complexes has an enantiotropic discophase. The [Pd{(C$_1$O)$_4$dpg}$_2$] complex does not exhibit a discophase. All of the transition temperatures of the complexes are plotted against the number of carbon atoms (n) in the alkoxy chains in Fig. 2. In this figure, the error bars denote the temperature range of the decomposition.

Enantiotropic Discotic Columnar Mesomorphism of [Pd{(C$_n$O)$_4$dpg}$_2$] (n=2—12). Each of the [Pd{(C$_n$O)$_4$dpg}$_2$] (n=2—12) complexes has an enantiotripic discophase. As can been from Fig. 3, the [Pd{(C$_{12}$O)$_4$dpg}$_2$] complex shows a fan-shaped texture at 220 °C upon cooling the isotropic liquid. A similar texture was observed for each of the [Pd{(C$_n$O)$_4$dpg}$_2$] (n=7—11) complexes. Generally, this texture is a characteristic of D$_{\text{hd}}$ mesophases.[13] The [Pd{(C$_n$O)$_4$dpg}$_2$] (n=2—6) complexes did not show any natural texture because of decomposition upon heating from room temperature.

The enantiotropic discophase of the [Pd{(C$_{12}$O)$_4$ dpg}$_2$] complex was also identified by X-ray diffraction measurement at room temperature (Fig. 4). The eight narrow peaks located at the lower angle region could be assigned to reflections from a two-dimensional

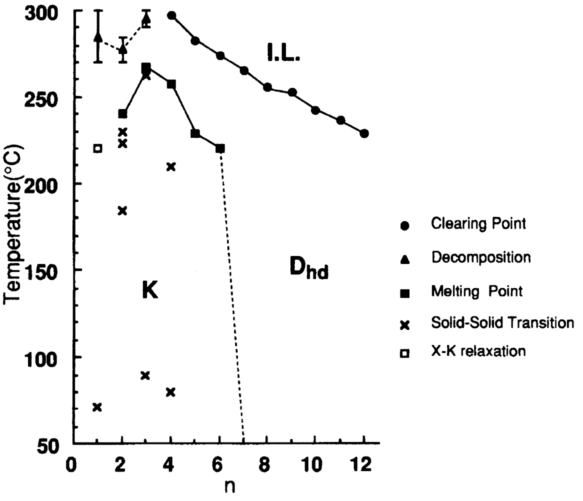

Fig. 2. Phase transition temperatures vs. the number of carbon atoms (n) in the alkoxy chains of the [Pd{(C$_n$O)$_4$dpg}$_2$] (n=1—12) complexes.

Table 2. Phase Transition Temperatures (T) and Enthalpy Changes (ΔH) of the [Pd{(C$_n$O)$_4$dpg}$_2$] (n=1—12) Complexes

n	Phase $\xrightarrow[\Delta H\ (\text{kJ mol}^{-1})]{T\ (°\text{C})}$ Phase[a)] $\rightsquigarrow$ Relaxation
1	$K_1 \xrightarrow{71} K_2 \xrightarrow{270\sim300} \text{Decomp.}$ $X \overset{\text{ca.220}}{\rightsquigarrow} K_2$
2	$K_1 \xrightarrow[{[2.38]}]{223} K_3$ $K_2 \xrightarrow[{[9.92]}]{184} K_3 \xrightarrow[{[1.98]}]{230} K_4 \xrightarrow[{[2.33]}]{240} D_{hd} \xrightarrow{270\sim285} \text{Decomp.}$ $D_{hd} \overset{\text{rapid cooling}}{\rightsquigarrow} K_2$
3	$K_1 \xrightarrow{\text{ca.95}} K_2 \xrightarrow{262} K_3 \xrightarrow{267} D_{hd} \xrightarrow{290\sim300} \text{Decomp.}$
4	$K_1 \xrightarrow{\text{ca.80}} K_2 \xrightarrow[{[2.15]}]{209} K_3 \xrightarrow[{[1.65]}]{258} D_{hd} \xrightarrow[{[32.8]}]{297} \text{I.L. (Decomp.)}$
5	$K \xrightarrow[{[9.54]}]{229} D_{hd} \xrightarrow[{[17.9]}]{283} \text{I.L. (Decomp.)}$
6	$K \xrightarrow[{[1.70]}]{220} D_{hd} \xrightarrow[{[26.3]}]{274} \text{I.L. (Decomp.)}$
7	$D_{hd} \underset{[24.8]}{\overset{265}{\rightleftarrows}} \text{I.L.}$
8	$D_{hd} \underset{[22.4]}{\overset{256}{\rightleftarrows}} \text{I.L.}$
9	$D_{hd} \underset{[27.2]}{\overset{253}{\rightleftarrows}} \text{I.L.}$
10	$D_{hd} \underset{[23.9]}{\overset{240}{\rightleftarrows}} \text{I.L.}$
11	$D_{hd} \underset{[24.5]}{\overset{236}{\rightleftarrows}} \text{I.L.}$
12	$D_{hd} \underset{[23.5]}{\overset{229}{\rightleftarrows}} \text{I.L.}$

a) Phase notation: K=crystal, X=unidentified disordered phase, D$_{\text{hd}}$=hexagonal disordered columnar mesophase, Decomp.=Decomposition, and I.L.=isotropic liquid.

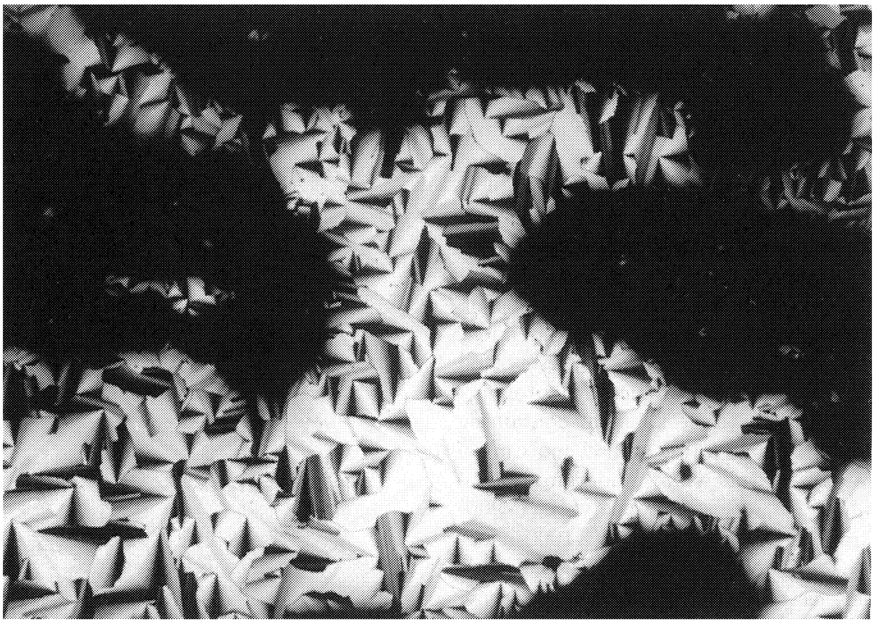

Fig. 3. Photomicrograph of the D_{hd} mesophase in the $[Pd\{(C_{12}O)_4dpg\}_2]$ complex at 220 °C.

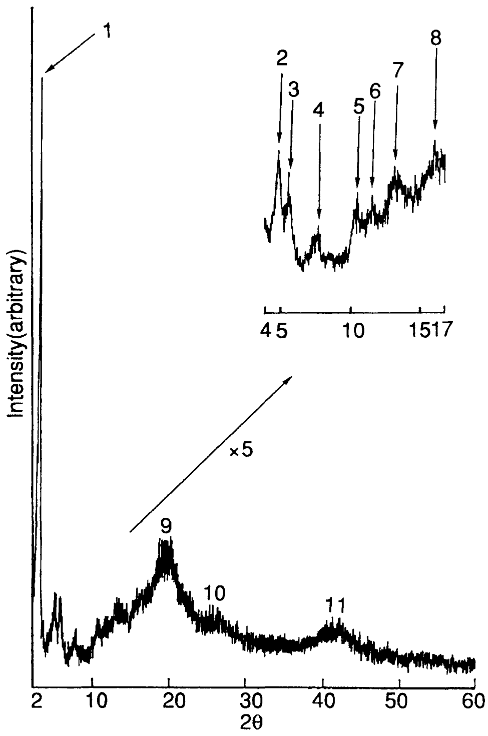

Fig. 4. X-ray diffraction pattern of the $[Pd\{C_{12}O)_4 dpg\}_2]$ complex at room temperature. See Table 3.

hexagonal lattice (Table 3). Hence, this discophase was assigned to a D_{hd} columnar mesophase. The other $[Pd\{(C_nO)_4dpg\}_2]$ (n=2—11) complexes gave the same assignment as that of the $[Pd\{(C_{12}O)_4dpg\}_2]$ complex. The lattice constants (a) of the two-dimensional hexagonal structures for the $[Pd\{(C_nO)_4dpg\}_2]$ (n=7—12) complexes are plotted against the number of carbon atoms (n) in the alkoxy chains in Fig. 5. A good linearity was observed between these lattice constant values and the number of carbon atoms (n).

Table 3. X-Ray Diffraction Data of the $[Pd\{(C_{12}O)_4 dpg\}_2]$ Complex at Room Temperature

Peak No.	Spacing (Å) d_{obsd}	Spacing (Å) d_{calcd}	Miller indices	Lattice constant (Å)
1	31.2	30.6	(100)	
2	17.7	17.7	(110)	
3	15.4	15.3	(200)	
4	11.3	11.6	(210)	a=35.4
5	8.29	8.50	(310)	
6	7.54	7.66	(400)	
7	6.59	6.68	(410)	
8	5.42	5.50	(510)	
9	ca. 4.6	—	Melting of alkoxy chains	
10	ca. 3.3	—	Fluctuation of interdisk distance	
11	ca. 2.3	—	The second halo of Peak 9	

Thermochromism. Interestingly, the $[Pd\{(C_nO)_4 dpg\}_2]$ complexes exhibit thermochromism. We examined in detail the thermochromism while taking the $[Pd\{(C_{12}O)_4dpg\}_2]$ complex as an example. The electronic spectra of the $[Pd\{(C_{12}O)_4dpg\}_2]$ complex have been measured at various temperatures (Fig. 6). As can be seen in this figure, the absorption band of 461 nm at 35 °C shifts to a higher energy (blue shift) and decreases in absorption intensity with increasing temperature; a new absorption band at around 400 nm gradually appears instead. This leads to thermochromism.

In a forthcoming paper[14] we will report that the bands of 461 nm, around 400 nm, and 267 nm at 35 °C could be assigned to the $4d_{z^2}$–$5p_z$ transition of Pd^{2+}

Table 4. Electronic Spectra Data of the [Pd{(C_{12}O)$_4$dpg}$_2$] Complex

Solvent	Dielectric constant at 20 °C	[Pd{(C_{12}O)$_4$dpg}$_2$] λ_{max}/nm	($\varepsilon\times10^4$)	Color
Hexane	1.89	269	(2.64)	Light orange
		332	(0.979)	
		365sh[a)]	(0.890)	
		461	(0.891)	
Carbon tetrachloride	2.238	278	(4.50)	Yellow
		390	(1.76)	
Benzene	2.283	279	(4.68)	Yellow
		390	(1.88)	
Chloroform	4.9	278	(4.90)	Yellow
		390	(2.00)	

a) sh=shoulder.

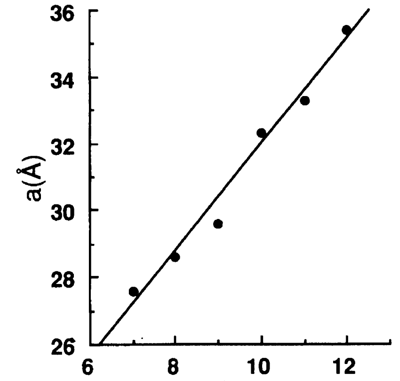

Fig. 5. Lattice constants a(Å) of the D_{hd} mesophases of the[Pd{(C_nO)$_4$dpg}$_2$] ($n=7$—12) complexes at room temperature vs. the number of the carbon atoms (n) in the alkoxy chains.

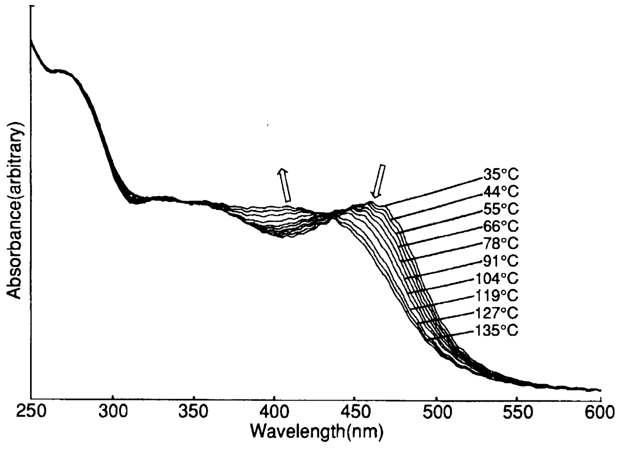

Fig. 6. Electronic spectra of a thin film of the [Pd{(C_{12}O)$_4$dpg}$_2$] complex at various temperatures.

(d–p band), the metal-to-ligand charge-transfer transition (MLCT band), and the π–π^* transition in the ligand, respectively. The bands at around 330 and 360 nm could not be assigned. It has been reported that the d–p band and MLCT bands shift to the lower energies (red shift) with increasing pressure,3—6,15) and that the d–p band is sensitive to the metal–metal distance. The decrease in the metal–metal distance with increasing pressure leads to piezochromism. Since the behavior of the MLCT band has not yet been studied, the mechanism of the blue shift of the MLCT band for the [Pd{(C_{12}O)$_4$dpg}$_2$] complex is ambiguous. However, it is probable that the blue shift of the d–p band for the [Pd{(C_nO)$_4$dpg}$_2$] complexes is due to an increase in the metal–metal distance, which can be explained as an excluded volume effect with increasing temperature. In fact, the average interdisk (metal–metal) distances which were measured by X-ray diffraction for the [Pd{(C_{12}O)$_4$dpg}$_2$] complex were 3.3 Å (at room temperature) and 3.5 Å (at 150 °C).

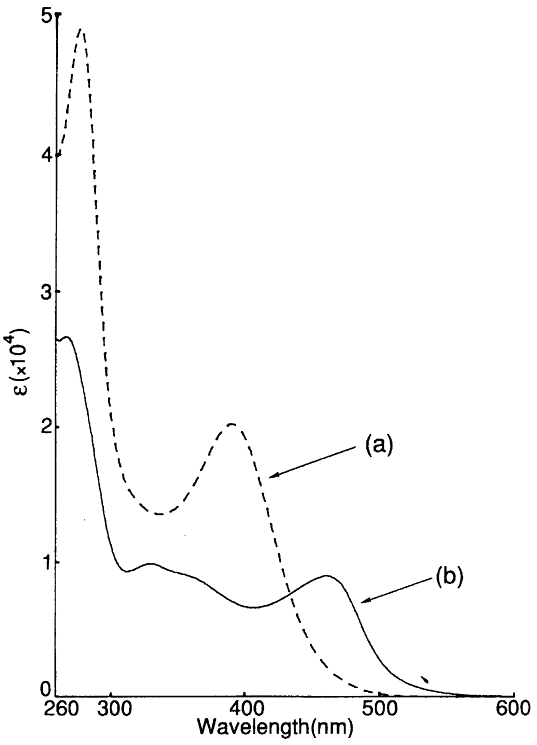

Fig. 7. Electronic spectra of the [Pd{(C_{12}O)$_4$dpg}$_2$] complex: (a) chloroform solution and (b) hexane solution. See Table 4.

Solvatochromism. The [Pd{(C_nO)$_4$dpg}$_2$] ($n=$

7—12) complexes swell and form orange gels in a concentrated hexane solution. On the other hand, when the hexane solutions of these complexes are dilute ($\leqq 4\times 10^{-5}$ mol dm^{-3}), gelation does not take place and the complexes result in a light-orange hexane solution. Other solutions in carbon tetrachloride, benzene, and chloroform of the complexes are yellow, althogh the concentrations of all the solutions are 4×10^{-5} mol dm^{-3} and almost the same as that of the hexane solution. We thus examined in detail the solvatochromism while taking the[$Pd\{(C_{12}O)_4dpg\}_2$] complex as an example. The electronic spectra of the hexane and chloroform solutions are shown in Fig. 7. As can be seen in this figure, these spectra are entirely different. Table 4 summarizes the electronic spectra data also involving the carbon tetrachloride and benzene solutions. The spectra of the solutions in carbon tetrachloride, benzene, and chloroform are almost the same.

When the spectra of the hexane and chloroform solutions in Fig. 7 where compared with that of the thin film shown in Fig. 6, the peak of 461 nm of the hexane solution corresponded to the d–p band. The peak of 390 nm of the chloroform solution is assigned to the MLCT band. The peaks of about 270 nm of both the hexane and the chloroform solutions are ascribed to the π–π^* transition in the ligand.

The electronic spectrum of the hexane solution in Fig. 7 was almost the same as that of the thin film at 35 °C in Fig. 6. In Fig. 6, the d–p band decreases in absorption intensity with increasing temperature, and the MLCT band gradually grows instead. It was found that the d–p band which was observed in the hexane solution disappeared in the other solutions. This leads to solvatochromism. This phenomenon will be reported in detail in a forthcoming paper.[14)]

References

1) Part XV: K. Ohta, Y. Morizumi, H. Akimoto, O. Takenaka, T. Fujimoto, and I. Yamamoto, *Mol. Cryst. Liq. Cryst.*, **214**, 143 (1992).

2) F. J. Welcher, "Organic Analytical Reagents." ed by D. Van Nostrand, New York (1947), Vol. 3, Chap. 6.

3) J. C. Zahner and H. G. Drickamer, *J. Chem. Phys.*, **33**, 1625 (1960).

4) M. Tkacz and H. G. Drickamer, *J. Chem. Phys.*, **85**, 184 (1986).

5) I. Shirotani, *Kino Zairyo* (in Japanese), **7**, 60 (1987).

6) I. Shirotani, *Gendai Kagaku* (in Japanese), **191**, No 2, 30 (1987).

7) K. Ohta, H. Hasebe, M. Moriya, T. Fjuimoto, and I. Yamamoto, *Mol. Cryst. Liq. Cryst.*, **208**, 43 (1991).

8) K. Ohta, H. Hasebe, M. Moriya, T. Fujimoto, and I. Yamamoto, *J. Master. Chem.*, **1**, 831 (1991).

9) H. Ema, Master Thesis, Shinshu University, Japan, Chap. 4, 1988.

10) U. T. Mueller-Westerhoff, A. Nazall. A. J. Cox, and A. M. Giroud, *Mol. Cryst. Liq. Cryst. (Lett.)*, **56**, 249 (1980).

11) H. Ema, Master Thesis, Shinshu University, Japan, Chap. 7, 1988.

12) H. Hasebe, Master Thesis, Shinshu University, Japan, Chap. 5, 1991.

13) C. Destrade, P. Foucher, H. Gasparoux, Nguyen H. T., A. M. Levelut, and J. Malthête, *Mol. Cryst. Liq. Cryst.*, **106**, 121 (1984).

14) K. Ohta, M. Moriya, M. Ikejima, H. Hasebe, T. Fujimoto, and I. Yamamoto, *Bull. Chem. Soc. Jpn.*, **66**, 3559 (1993).

15) K. Shirotari, K. Suzuki, T. Suzuki, T. Yagi, and M. Tanaka, *Bull. Chem. Soc. Jpn.*, **65**, 1078 (1992).